Measuring the Coordination Number and Entropy of a 3D Jammed Emulsion Packing by Confocal Microscopy

Jasna Brujić
Department of Physics and Center for Soft Matter Research, New York University, New York, New York 10003, USA

Chaoming Song, Ping Wang, Christopher Briscoe, Guillaume Marty, and Hernán A. Makse
Department of Physics and Levich Institute, City College of New York, New York, New York 10031, USA
(Received 14 April 2006; revised manuscript received 26 November 2006; published 15 June 2007)

Jammed matter is by definition impenetrable to light, such that little is known about the geometry of jammed systems. Using confocal microscopy to image an emulsion in 3D, we first explain the origin of the enhanced fluorescence at the droplet contacts and then determine the contact network inside the model frictionless system. This enables the experimental determination of the average coordination number $\langle Z \rangle$ which agrees with the isostatic predicted value of $\langle Z \rangle \approx 6$. Furthermore, we calculate the entropy of the packing from the network of contacts.

DOI: 10.1103/PhysRevLett.98.248001 PACS numbers: 45.70.Cc, 87.64.Tt

Pouring sugar into a cup is the simplest example of a fluid to solid transition, which takes place because of an increase in the density, identified as the jamming transition [1]. If the particles are deformable, the applied stress is also an important control parameter for jammed systems as the density increases with the applied load [2]. The density is high enough to support an external weight at the isostatic limit, when the particles have enough contacts between them such that all the forces balance according to Newton's equations [3]. The average number of contacts per particle, $\langle Z \rangle$, known as the coordination number, is therefore the key parameter that determines the mechanical properties of granular materials. Theory predicts that a system of frictionless spherical particles has a minimal average number of contacts for mechanical stability $\langle Z \rangle = 2D$ [4], where D is the dimension of the system.

The problem with jammed matter, from sand piles to mayonnaise, is that it is difficult to take a look inside the particulate packing to measure Z. Indeed, in the old days Mason, a postgraduate student of Bernal, took on the task of shaking glass balls in a sack and ''freezing'' the resulting configuration by pouring wax over the whole system. He would then carefully take the packing apart, ball by ball, noting the positions of contacts for each particle [5]. Since this labor-intensive method patented half a century ago, yet still used in recent studies [6], other groups have extracted data at the level of the constituent particles using x-ray tomography [7]. However, neither method could directly determine the contacts in order to be sure whether the particles were touching or just very close together. Moreover, these methods only provide insight into large particles and do not lend themselves to the exploration of jammed matter on the colloidal length scale. Given the recent theories unifying the concepts in granular materials and glasses [1], the characterization of all jammed matter is important for the advancement of this field.

In this Letter, we explain a different method which directly highlights the contacts between droplets in a dyed jammed emulsion. While previous experiments were based on the visualization of the areas of droplet deformation [8,9], here we explain the origin of the enhanced fluorescence at the contacts in terms of the polarity of the environment of the dye. Since the dye has amphiphilic character it preferentially sits at the oil-water interface, where its emission wavelength band is blueshifted compared to the emission of the same dye in the oil droplet core. As two droplets touch on length scales below the resolution of the microscope, the concentration of these interfacial dye species increases, giving rise to highlighted areas of contact that can then be identified. This information allows for the reconstruction of the contact network for any external pressure of the system, in particular, that of the low pressure isostatic limit. Using a combination of UV-Vis spectroscopy and fluorescence microscopy we present a measurement of $\langle Z \rangle$ for a frictionless jammed material and a measurement of the entropy in jammed systems on the colloidal length scale.

Emulsion system.—The model system consists of fluorescently labeled silicone oil droplets with Nile red dye, suspended in a solution of 1:1.05 water to glycerol volume ratio to ensure refractive index matching [8]. This emulsion system is stabilized by sodium dodecyl sulfate (SDS) surfactant, at 10 mM concentration, i.e., below the critical micellar concentration (CMC), thus avoiding depletion attraction between the droplets [10]. A crude emulsion was first made by rapid mixing of the two phases in the presence of surfactant, after which the droplet size distribution was refined using the narrow gap shear method [11] to yield a radius distribution of 2 ± 0.7 μm, shown in Fig. 1. The emulsions were characterized using a laser scanning confocal microscope (LSCM, Zeiss). The droplet radii were measured with subvoxel accuracy from the 3D

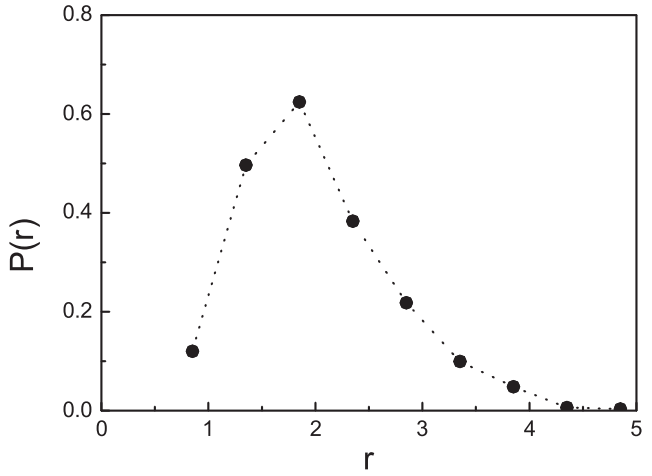

FIG. 1. Radius distribution of 1869 emulsion droplets, obtained from a Fourier Transform 3D image analysis of the confocal microscope images, shown in Fig. 2.

confocal images containing 1869 droplets using image analysis techniques developed in [8]. The emulsion serves as a model for a granular material composed of soft spheres, which can be considered frictionless due to the lubrication by the continuous phase fluid.

Method.—The activity of Nile red dye depends on its environment, such that the fluorescence of different regions of the sample are observed in different spectral domains. The imaging method thus consists of exciting the dye at a wavelength of 488 nm and splitting the emitted signal into two channels, CH1 and CH2, as shown in Fig. 2. This separates the droplet cores from their interfaces in the fluorescence signal, while the continuous phase gives no significant emission. The superposition of the two channels gives rise to images where areas of contacts between droplets are highlighted, as shown in Fig. 2(c). Since the analysis method is based on this increased fluorescence as two interfaces get closer than the microscope resolution, one needs to distinguish between neighboring interfaces and true droplet deformations due to contact forces. We therefore compress the emulsion by centrifugation at 6000 g, such that the average pressure on each droplet is $\sigma = 4.5$ Pa, causing an average interdroplet force of $\bar{f} =$ 15 nN. Pressures in this range cause exponentially distributed areas of deformation in the droplet packing (data not shown), much larger than those created by neighboring droplets below the resolution limit, thus minimizing the error in contact estimation. This method then facilitates a complete study of the contact network in a 3D sample.

Environment-sensitive fluorescence of Nile red.—We now describe the UV-visible spectrometer experiments showing that the fluorescence of Nile red depends on its environment. We first consider the emission spectra of the emulsion system with varying proportions of the different components, i.e., the aqueous phase, the droplets and the interfaces. This is achieved by making emulsions at different volume fractions. The size distribution remains the

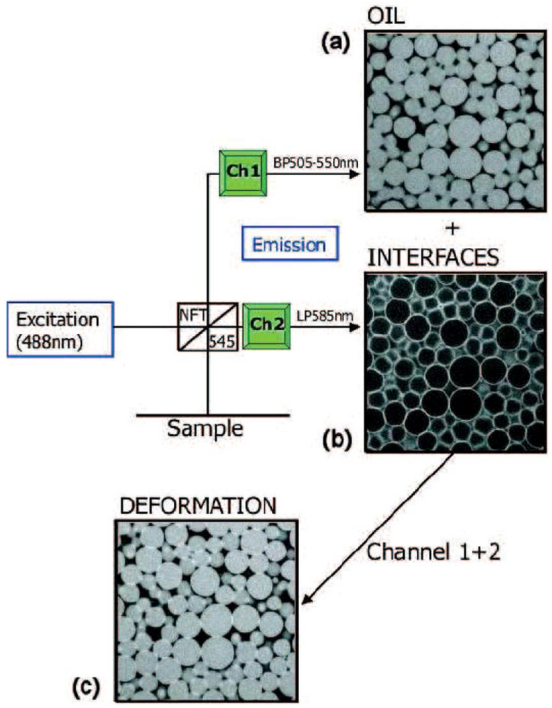

FIG. 2 (color online). Confocal microscope images obtained by splitting the fluorescence using optical filters, (a) BP505-550 nm and (b) LP585 nm, and their subsequent superposition (c) providing the contrast necessary for image analysis of droplet contacts. Note that contacts are highlighted.

same between the measurements since we use the same stable emulsion system that does not coarsen on a time scale of months. The results are presented in Fig. 3, for volume fractions ranging from $\phi = 0$ (purely aqueous phase) to $\phi = 0.75$. The peak corresponding to the continuous phase alone at $\phi = 0$ is located around $\lambda =$ 640 nm. As the droplet volume fraction is increased, two effects are observed. First, a peak at shorter wavelengths

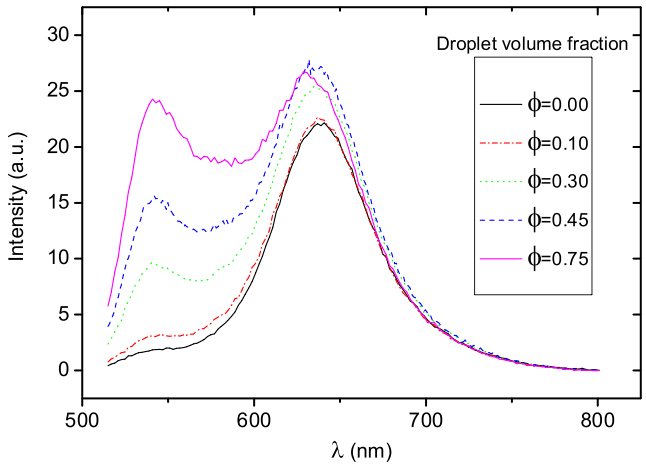

FIG. 3 (color online). Emulsion UV-vis emission spectra for different droplet volume fractions from $\phi = 0$–0.75. This demonstrates the environment-sensitive fluorescence of Nile red.

around 545 nm becomes apparent and grows linearly with the volume fraction. This peak can be attributed to the fluorescence from the oil phase, as confirmed by the spectra of Nile red in pure oil. Second, the peak at $\lambda = 640$ nm increases by 22% between $\phi = 0$ and $\phi = 0.75$, whereas the proportion of the aqueous phase actually decreases as more droplets are added. This increase must therefore be due to the increase in the number of interfaces as more droplets are added. The emission band of the interface regions is interestingly the same as that of the continuous phase and shifted from that of the droplet cores. To explain this, we study the emission spectra of only the aqueous phase for increasing SDS concentrations, as shown in Fig. 4(a). The drastic fluorescence enhancement, particularly above the CMC, suggests that micelles play a crucial role in the solubilization of the dye. This is due to the amphiphilic character of the dye molecules, which favor interfacial regions over hydrophobic regions or water. They can achieve this conformation either in the micelles in the aqueous phase or the oil-water interface, as schematically represented in Fig. 4(b) [12]. These environments are therefore locally of the same polarity. The fact that interfaces appear 8 times brighter than the continuous phase in the spatially resolved confocal microscope images, see Fig. 5, can be attributed to the much higher concentration of dye molecules that are localized at the surface of each droplet, as compared to the few dye molecules that are diffusing in micelles in the continuous phase.

On the other hand, Nile red molecules in the purely hydrophobic cores of the droplets experience a blueshifted, weaker emission since their environment is nonpolar. Having explained the method and its underlying mechanism, we now turn to the interesting possibilities it raises. It has already been applied to the study of force distributions in such systems [8], and here we expand the method to focus on the network of contacts.

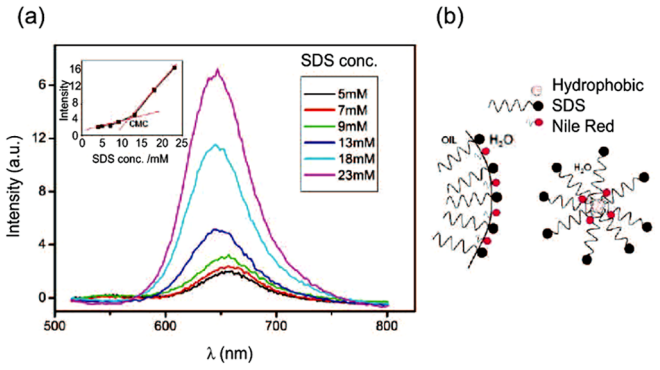

FIG. 4 (color online). (a) Emission spectra of the aqueous phase at a constant Nile red concentration, but increasing SDS concentration. The maximum intensity is plotted versus the SDS concentration in the inset, showing a change of behavior at a concentration which corresponds to the CMC. (b) Schematical representation of Nile red insertion at the interfaces (right) and in micelles (left).

Average coordination number.—From the detection of contacts we now compute the average number of contacts per particle. With N frictionless particles in dimension D, one has ND Newton equations and $N\langle Z\rangle/2$ unknowns corresponding to the normal forces between droplets. For the system to be solvable, it requires $\langle Z\rangle = 2D$. In 3 dimensions, this leads to $\langle Z\rangle = 6$, the isostatic limit. Experiments to measure this coordination number have been performed on grains. For instance, Bernal [5] found $\langle Z\rangle = 6$, while for frictional grains the prediction is $\langle Z\rangle = D + 1 = 4$ [2]. Additionally, molecular dynamics simulations have shown that $\langle Z\rangle$ can be a function of the friction coefficient, reducing smoothly from 6 as friction is introduced [13]. It is therefore interesting to measure this quantity in a truly frictionless case. We employ a 3D image analysis technique to measure the droplet radii and positions with subvoxel accuracy, as well as the contact areas between those droplets that exert forces on one another. Because of the polydispersity of the system, the droplet volume fraction for six such images is calculated to be $\phi = 74\%$ at the applied pressure of $\sigma = 4.5$ Pa per droplet. We identify an inner window where all the neighboring droplets have been identified and run a coordination number analysis on 1544 such droplets. A contact is considered when the area of deformation is larger than the resolution limit of the technique.

The distribution of Z is represented in Fig. 6(a). The mean value extracted from this distribution is $\langle Z\rangle = 6.08$, in close agreement with the theoretical value of 6. The slight excess of contacts can be attributed to the pressure exerted on the system. Note that the distribution $P(Z)$ exhibits an exponential tail due to the polydispersity of the particles which enables a more efficient packing, but despite this large polydispersity, the average value of 6 still holds. This provides experimental evidence for the prediction $\langle Z\rangle = 2D$, for the case of frictionless particles at the colloidal length scale.

Entropy considerations.—We next compute the entropy of the jammed system from microscopic variables such as the droplet contacts. Determining the entropy through the statistics of volumes, as suggested in numerous theoretical works [14,15], would require the knowledge of the density of states, which is still an open issue. We therefore use an alternative method that characterizes the states of the sys-

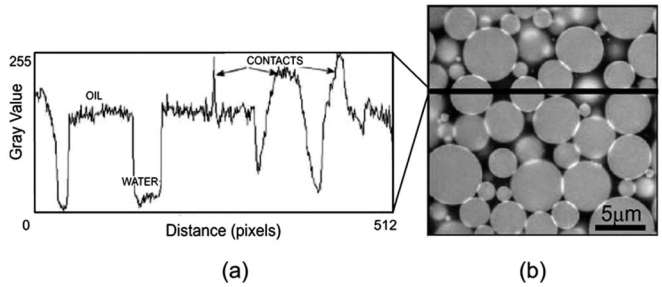

FIG. 5. (a) Intensity profile along the black line of image (b), indicating the enhancement at the droplet contacts.

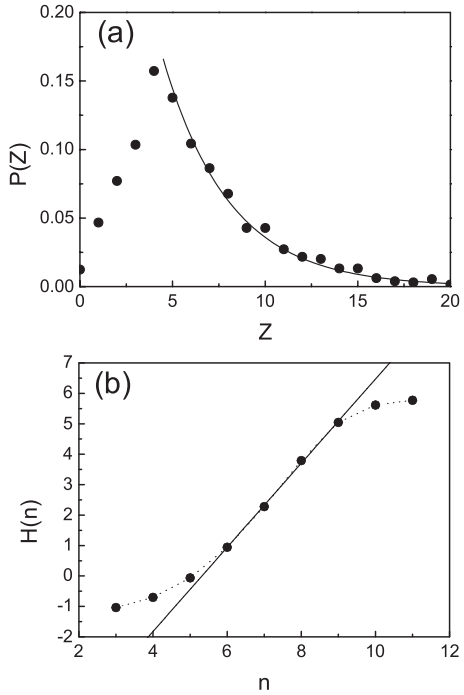

FIG. 6. (a) Distribution of the number of contacts per particle, Z. The mean value is $\langle Z \rangle = 6.08$. The solid line is an exponential fit of the tail of the distribution. (b) H as a function of the cluster size n.

tem using graph theoretical representations and we compute the entropy density s using information theory (Shannon entropy) [16,17]. To achieve this, we use our knowledge of the contact positions to build the corresponding network. In this representation, a cluster of n droplets is simply a graph which, by means of graph automorphism [18], can be transformed into a standard form (also known as "class") so that two topologically equivalent graphs belong to the same class. A given class i can then be considered as a state with an occurrence $p(i)$. In practice, one can determine $p(i)$ by extracting a large number m of clusters of size n from the system and counting the number of times f_i a cluster i is observed, so that

$$p(i) = \frac{f_i}{m}. \tag{1}$$

This allows us to compute the entropy corresponding to clusters of size n

$$H(n) = -\sum p(i) \ln p(i), \tag{2}$$

where i runs over all possible clusters of size n, and where we assume that the equivalent of the Boltzmann constant is $\lambda = 1$. Using information theory, the entropy density s is then calculated as follows

$$s = \lim_{n\to\infty} [H(n+1) - H(n)]. \tag{3}$$

With the values of $p(i)$ and Eqs. (2) and (3), it is then possible to determine s. It converges rapidly so that even moderate values of n are enough to obtain a good approximation of s, as shown in Fig. 6(b). At large n, H clearly suffers finite size effects, but the existence of a linear regime for intermediate values of n (between $n = 6$ and 10) demonstrates the rapid convergence of Eq. (3), at lower n than has recently been observed in two-dimensional granular materials [19]. This indicates that entropy is an extensive property and the entropy density is constant and well defined. The entropy per grain is then given by the slope of the linear section of the graph, giving $s \simeq 1.4$ (in units of λ).

To conclude, we demonstrated a neat experimental technique for getting through a jammed system in a matter of seconds, giving direct access to contact positions. This method opens the way to study packings as a function of volume fraction, in order to reach an equation of state for jammed systems [2].

We thank Sam F. Edwards, I. Hopkinson, and H. Zhang for discussions and the Cavendish Laboratory at the University of Cambridge where part of this work was performed. We acknowledge support from DOE, NSF-CMMT, and NSF-CREST. J. B. was supported by the Burroughs Wellcome Fund.

[1] *Unifying Concepts in Granular Media and Glasses*, edited by A. Coniglio, A. Fiero, H. J. Herrmann, and M. Nicodemi (Elsevier, Amsterdam, 2004).
[2] H. A. Makse, D. L. Johnson, and L. M. Schwartz, Phys. Rev. Lett. **84**, 4160 (2000).
[3] S. F. Edwards and D. V. Grinev, Phys. Rev. Lett. **82**, 5397 (1999).
[4] S. Alexander, Phys. Rep. **296**, 65 (1998).
[5] J. D. Bernal and J. Mason, Nature (London) **188**, 910 (1960).
[6] A. Donev *et al.*, Science **303**, 990 (2004).
[7] P. Richard *et al.*, Phys. Rev. E **68**, 020301 (2003).
[8] J. Brujić *et al.*, Physica (Amsterdam) **327A**, 201 (2003).
[9] J. Zhou, S. Long, Q. Wang, and A. D. Dinsmore, Science **312**, 1631 (2006).
[10] T. G. Mason, J. Bibette, and D. A. Weitz, Phys. Rev. Lett. **75**, 2051 (1995).
[11] C. Mabille *et al.*, Langmuir **16**, 422 (2000).
[12] B. D. Wagner *et al.*, J. Inclusion Phenom. **45**, 275 (2003). (1989).
[13] L. Silbert *et al.*, Phys. Rev. E **65**, 031304 (2002).
[14] S. F. Edwards and R. B. Oakeshott, Physica (Amsterdam) **157A**, 1080 (1989).
[15] R. Blumenfeld and S. F. Edwards, Phys. Rev. Lett. **90**, 114303 (2003).
[16] C. E. Shannon, Bell Syst. Tech. J. **27**, 379 (1948).
[17] R. L. C. Vink and G. T. Barkema, Phys. Rev. Lett. **89**, 076405 (2002).
[18] B. D. McKay, *Nauty User's Guide (version 1.5)* (Australian National University, Canberra, 1990), Tech. Rep. TR-CS-90-02.
[19] F. Léchenault, O. Dauchot, and E. Bertin, J. Stat. Mech. (2006) P07009.